



Histone acetylation-mediated regulation of genes in leukaemic cells

A.E. Chambers^{a,*}, S. Banerjee^b, T. Chaplin^a, J. Dunne^a, S. Debernardi^a,
S.P. Joel^a, B.D. Young^a

^a*Cancer Research UK Medical Oncology Laboratory, The Medical College of St. Bartholomew's Hospital,
Charterhouse Square, London, EC1M 6QB, UK*

^b*Harris Birthright Research Centre for Fetal Medicine, King's College Hospital Medical School,
Denmark Hill, London SE5 8RX, UK*

Received 30 July 2002; received in revised form 2 December 2002; accepted 13 January 2003

Abstract

Histone deacetylase (HDAC) and histone acetyltransferase (HAT) functions are associated with various cancers, and the inhibition of HDAC has been found to arrest disease progression. Here, we have investigated the gene expression profiles of leukaemic cells in response to the HDAC inhibitor trichostatin A (TSA) using oligonucleotide microarrays. Nucleosomal histone acetylation was monitored in parallel and the expression profiles of selected genes were confirmed by quantitative polymerase chain reaction (PCR). A large number of genes (9% of the genome) were found to be similarly regulated in CCRF-CEM and HL-60 cells in response to TSA, and genes showing primary and secondary responses could be distinguished by temporal analysis of gene expression. A small fraction of genes were highly sensitive to histone hyper-acetylation, including *XRCC1*, *HOXB6*, *CDK10*, *MYC*, *MYB*, *NMI* and *CBFA2T3* and many were trans-acting factors relevant to cancer. The most rapidly repressed gene was *MKRN3*, an imprinted gene involved in the Prader–Willi syndrome.

© 2003 Elsevier Science Ltd. All rights reserved.

Keywords: Leukaemia; Acetylation; Histone; Gene; Regulation; Microarrays

1. Introduction

Histone modification is emerging as a central theme in the regulation of gene expression in a variety of cancers. A dynamic equilibrium of histone acetyltransferase (HAT) and histone deacetylase (HDAC) functions control the level of acetylated histones in nuclear chromatin. HATs activate genes by altering chromatin configuration, facilitating transcription factor access, while HDACs have the opposite effect, mediating transcriptional repression [1]. Mammalian HDACs are grouped into three classes (I–III), according to homology with their yeast counterparts [2]. Both class I and class II mammalian enzymes are sensitive to the inhibitor, trichostatin A (TSA), while class III HDACs are insensitive due to

the absence of the Zn^{++} -requiring catalytic site that is shared by the class I and II enzymes. Abnormal expression, function or recruitment of HDACs is associated with neoplasia, including lymphoid and myeloid leukaemias, and the use of HDAC inhibitors can arrest tumour progression [3–8].

Histone deacetylases form repressor complexes (pRb, NuRD and Sin3) with transcription activators (e.g. E2F) and with other HDACs [9,10]. The NuRD and Sin3 complexes are important in several types of leukaemia [11]. In acute promyelocytic leukaemias (APL), fusion of genes encoding transcriptional regulators with the retinoic acid receptor gene give rise to mutant fusion proteins that recruit HDAC/Sin3 complexes and mediate target gene repression, preventing cellular differentiation. In most types of APL, this repression can be relieved by treatment with retinoic acid. However, in Promyelocytic Leukaemia Zinc Finger-Acute Myeloid Leukaemia (PLZF-AML), the repression complex cannot be disrupted by retinoic acid alone and there is an absolute requirement for HDAC inhibition in order to

* Corresponding author at Present address: Department of Dermatology, San Francisco General Hospital, 1001 Potrero Street, Building 100, Room 269, University of California, San Francisco, CA 94110, USA. Tel.: +1-415-647-3992; fax: +1-415-647-3996.

E-mail address: annechambers@yahoo.co.uk (A.E. Chambers).

achieve differentiation [3]. Differentiation therapy using HDAC inhibitors is currently under investigation as a treatment for acute myeloid leukaemias [4].

HDACs are crucial for haemopoiesis and are recruited via the Ikaros family of transcription factors to modulate gene expression during differentiation [12–14]. The recruitment of HDACs by faulty co-repressors is found in many haemopoietic cancers [15], including acute and T-cell acute lymphoblastic leukaemias [13,14].

2. Materials and methods

2.1. Cell culture

CCRF-CEM (T lymphoblastoid) and HL-60 (promyelocytic cells) were grown in Roswell Park Memorial Institute (RPMI) 1640 medium containing 2 mM L-glutamine, 10% (v/v) fetal calf serum and 20 units/ml penicillin/streptomycin. Trichostatin A (Sigma, St. Louis, MO, USA) was dissolved in ethanol at a concentration of 1 mg/ml. Cells ($0.25\text{--}1 \times 10^9$ at $0.5\text{--}2 \times 10^7$ /ml) were harvested either before or 0.25, 1, 2, 4, 6, 8, 14, 16 and 24 h after treatment with 1.5 μM TSA, and used to extract RNA or histones.

2.2. Extraction of acetylated histones and gel electrophoresis

Histones from TSA-treated and untreated CCRF-CEM and HL-60 cells (10^8 cells) were prepared as described in Ref. [16]. Briefly, cells were harvested, washed in ice-cold buffer (150 mM KCl, 20 mM Hepes, pH 7.9, 0.1 mM ethylene diamine tetra acetic acid (EDTA), 2.5 mM Mg^{2+}) and Dounce homogenised (12 strokes, loose pestle) in ice-cold buffer containing 250 mM sucrose and 1% (v/v) Triton X100. Nuclei were recovered by centrifugation, washed, and proteins were extracted for 1 h using 0.25 M HCl. Chromosomal proteins were precipitated with 20% (w/v) trichloroacetic acid (TCA), washed once with cold acidified acetone and twice with cold acetone before resolving in 15% (w/v) acid-urea-Triton (AUT) gels using calf thymus histones (Worthington Biochemical Corporation, NJ, USA) or HeLa histones as standards. The AUT gels were as described in Ref. [17]. Gels were prerun at 12 mA (constant current) for 30 min prior to loading. Approximately 10–15 μg of protein was loaded per track. Electrophoresis was at 8 mA for 16–18 h; gels were stained with Coomassie blue and photographed.

2.3. Preparation of RNA

TSA-treated and untreated CCRF-CEM and HL-60 cells (approximately 10^8 cells per treatment time point) were homogenised in RLT buffer (Qiagen, Chatsworth,

CA, USA) containing β -mercaptoethanol, and total RNA was purified using RNeasy columns (Qiagen). The integrity of the RNA was verified by electrophoresis through denaturing agarose gels. RNA for quantitative polymerase chain reaction (PCR) was further treated with RQ1 RNase-free DNase to remove the residual DNA. Following heat-inactivation of DNase, RNA was phenol/chloroform extracted and ethanol precipitated with 20 μg glycogen (Boehringer Mannheim).

2.4. Microarrays

Total RNA (10–20 μg) was used to synthesise biotinylated cRNA for hybridisation to Affymetrix U95A Ver2 oligonucleotide microarrays according to the supplier's protocol (Affymetrix, Santa Clara, CA, USA). Briefly, RNA was annealed to 100 picomoles of T7-(dT)₂₁ primer; TCTAGTCGACGGCCAGTGAA TACGACTCACTATAGGGCGTTTTTTTTTTTTTTTTTTTT (MWG Biotech AG, Milton Keynes, UK) and double-stranded cDNA was synthesised using a SuperScript ds-cDNA synthesis kit (Life Technologies, Paisley, UK). Biotin-labelled copy RNA was synthesised using an Enzo BioArray High Yield RNA Transcript Labelling Kit (Enzo Diagnostics Inc., Farmingdale, NY, USA) via *in vitro* transcription with T7 RNA polymerase. The hybridisation mixture contained biotinylated fragmented cRNA (15–20 μg), commercially prepared control cRNAs (GeneChip Eukaryotic Hybridisation Control Kit; Affymetrix), herring sperm DNA and acetylated bovine serum albumin (BSA) according to the manufacturer's recommendations. GeneChips were hybridised for a maximum of 16 h at 45 °C, and washed according to the suggested protocol for standard arrays (Affymetrix). Hybridisation signals were detected by streptavidin phycoerythrin staining and the signal amplified using a biotinylated anti-streptavidin antibody, followed by further streptavidin phycoerythrin staining. Microarrays were scanned using GeneChip software (Affymetrix Microarray Suite version 5). The scans were normalised on the basis of a linear scaling method such that the average value of every array was adjusted to a common value (target intensity or TGT) of 100, to account for different chip intensities, and a relative measure of abundance was assigned to the corresponding transcripts.

2.5. Microarray data analysis

GeneSpring version 4.1 (Silicon Genetics, Redwood City, CA, USA) was used for data analysis. All arrays were normalised using the 50th percentile of all measurements as a positive control for each sample; the measurement for each gene was divided by this synthetic positive control, assuming that this was at least 10. The bottom 10th percentile was used as a test for correct

background subtraction. This was never less than the negative of the synthetic positive control. The measurement for each gene in each sample was divided by the corresponding value in the 0 h chip in the respective cell line. The control channel value for each gene for each sample was used as a measurement of trust. Data trust is a measure of the reliability of the data and was calculated as the product of the median value of the chip and the average of the gene's measurement in the control sample. Control channel values below 0.0 were considered as bad data points.

Affymetrix U95A version 2 GeneChips represent approximately 12 000 arrayed genes. Data from the two cell lines were compared and genes showing a cell type-specific response to histone hyper-acetylation were removed. *MYC*, an important responder to TSA [18] showed no more than 10.6% variation in expression at any given time point, between the two cell lines. Therefore, we decided to restrict the allowable variation between the two cell lines to 10.6% and genes which varied more than *MYC* in their expression between cell lines at analogous time points were removed, resulting in a basic gene set of 4495 genes. This gene set was further filtered to remove genes varying less than 2-fold in either or both cell lines, resulting in a set of 1099 genes from which genes varying more than 5-, 8- and 10-fold were identified. Hierarchical clustering was performed using the Pearson correlation metric on the \log_{10} of the ratio using the TREE program of GeneSpring 4.1.

2.6. Quantitative PCR

DNase-treated RNA (250 ng) from the TSA time course experiments was reverse transcribed using SuperScript II RT (Life Technologies, Paisley, UK). With the exception of 6 h TSA CCRF-CEM for which there was insufficient RNA, all time points represented in the microarray were used in the quantitative PCR. The expression patterns of two genes (*HOXB6* and *NMI*) were examined. *ACTB* (β -actin, GenBank accession No. X00351) was chosen as an internal control, since its expression variation throughout the TSA time course in both CCRF-CEM and HL-60 cells was minimal. Both *HOXB6* and *ACTB* primers corresponded to the area of the gene represented on the U95A ver2 microarray chip. Optimal primer pairs were designed using GeneFisher (<http://bibiserv.techfak.uni-bielefeld.de/genefisher/>). Primer pairs were as follows: *ACTB*; forward, AGCATCCCCCAAAGTTCACA; reverse, TGTG TGGACTTGGGAGAGGA. *HOXB6*; forward, CTTC CTGGTGAGAACTGAGGA; reverse, CTGAGGAC AGCGAATCTACCA. *NMI*; forward, TCTAAGA GGACAGTGCTTCTGA; reverse, TGACCTAGAGA ACACTTGACCA. Specific primers for each gene were used to amplify equal amounts (5 ng) of each first strand cDNA in triplicate via quantitative PCR using

the ABI 7700 Sequence Detection System with SYBR Green PCR Master Mix (Applied Biosystems, Foster City, CA, USA). Affymetrix Microarray Suite version 5 microarray data for *ACTB*, *HOXB6* and *NMI* were removed from the Excel file and analysed separately in Excel in an identical manner to data generated by quantitative PCR. Both sets of data for each gene were normalised to one time point in the respective cell line and all points in each gene were normalised to the respective (either microarray or quantitative PCR generated) *ACTB* (β -actin) data. In the CCRF-CEM TSA time series, *HOXB6* was undetectable at 0 h, therefore microarray and PCR data for this gene and the *ACTB* gene were normalised to the 4 h TSA time point. For the *NMI* gene and *ACTB* in the CCRF-CEM TSA time series, microarray and PCR data were normalised to the 0 h time point. In the HL-60 TSA time series, microarray and PCR data for the *NMI* and *ACTB* genes were normalised to the 0.25 h TSA time point, and for the *HOXB6* and *ACTB* genes were normalised to the 0 h time point. Each reaction was done in triplicate in three or more experiments. Triplicate data from each experiment on a single 96-well PCR plate were analysed separately using standard curves for each gene according to the manufacturer's recommendations (Applied Biosystems, Foster City, CA, USA).

3. Results

3.1. HDAC inhibition monitored by analysis of histone hyper-acetylation

Inhibition of histone deacetylases with trichostatin A results in histone hyper-acetylation that is dependent on the drug concentration and time. However, cell lines and cell types show variation in their response to TSA [8,19]. In order to determine a saturating dose and time scale of incubation for gene expression profiling by microarray analysis, the acetylation state of nuclear histones in response to TSA was monitored by electrophoresis through AUT gels. A concentration of 1.5 μ M TSA was found to induce maximum histone hyper-acetylation and was used in all further experiments. CCRF-CEM and HL-60 cells were incubated with 1.5 μ M TSA for up to 48 h (Fig. 1 and data not shown). The acetylation state of H4 and H2B histones in untreated cells was similar in both cell types; histone H4 was predominantly un-acetylated and mono-acetylated, while most of the histone H2B was un-acetylated. Both cell types responded similarly to TSA treatment; at 2 h, there was a significant increase in the levels of di-, tri- and tetra-acetylated histone H4 with a concomitant stoichiometric reduction of un-acetylated and mono-acetylated forms. The accumulation of tetra-acetylated histone H4 was complete by 14 h (Fig. 1a), and was

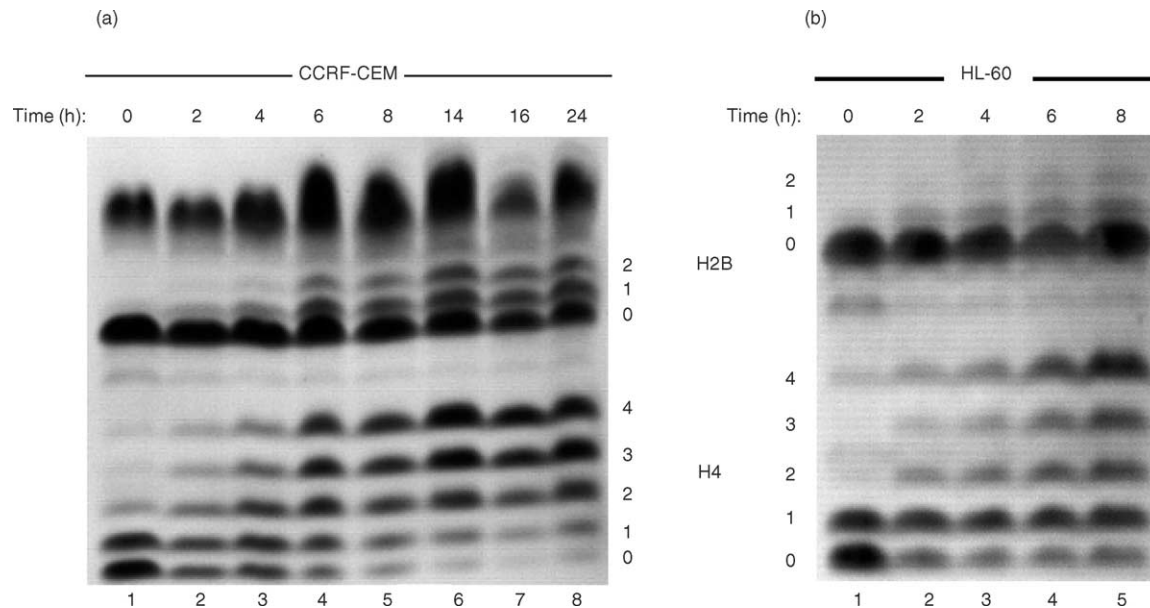


Fig. 1. Time-dependent hyper-acetylation of histone H2B and H4 in response to trichostatin A (TSA). (a) Time course analysis of histone acetylation in CCRF-CEM cells. (b) Time course analysis of histone acetylation in HL-60 cells. Nuclear proteins (10 µg/track) from untreated and trichostatin A (1.5 µM)-treated cells were extracted and resolved on 15% (w/v) polyacrylamide acid urea Triton (AUT) gels. Only the relevant portions of the gels are shown. Track 1 (a and b), no treatment control; tracks 2–5 (a and b) at 2, 4, 6 and 8 h incubation with TSA respectively; tracks 6–8 (a only) at 14, 16, and 24 h incubation with TSA, respectively. The five acetylation states of histone H4 are labelled (0–4), representing un-acetylated, mono-, di-, tri- and tetra-acetylated forms. Similarly, three different acetylated forms of H2B are indicated.

unchanged on further incubation (> 14 h; Fig. 1a and data not shown), indicating that maximum histone H4 hyper-acetylation is achieved between 8 and 14 h. The rate of change of acetylation in both cell types was greatest between 0 and 8 h (Fig. 1), suggesting that transcription from genes that are sensitive to changes in histone acetylation and localised structural transitions of chromatin, might be altered within this time frame.

3.2. Gene expression profiling

Given that the maximum rate of change in acetylation occurred between 0 and 8 h (Fig. 1), and that significant acetylation was observed by 2 h, microarray analysis was performed on RNA extracted from cells incubated for 0 to 8 h with TSA; specifically, 0, 0.25, 1, 2, 4, 6 and 8 h. By analysing the early time points, alterations in the expression of genes that have an immediate early response to histone hyper-acetylation may be detected. These early changes in gene products might alter a secondary set of genes by activation or repression *in trans*. Additionally, inhibition of the deacetylation of non-histone substrates could potentially influence immediate early gene expression.

Since we aimed to identify common TSA target genes rather than examine the overall expression patterns of a particular cell type, the response profiles of cells derived from very different leukaemias were compared. This provided a more stringent replication of the experimental data that obviated the need for repetition at the

level of the individual cell lines. Our data analysis involved a stepwise comparison of the two cell lines throughout the time course (see Section 2). While it is likely that genes whose expression is modulated by changes in histone acetylation could have been lost via this analysis, it is unlikely that the reverse holds true (aberrant inclusion of genes not modulated by histone acetylation).

3.3. Identification of a large number of TSA-responsive genes that have common expression profiles in CCRF-CEM and HL-60 cells

Approximately 4495 genes showed consistent expression in the two cell lines in response to TSA (Fig. 2 and data not shown). These genes followed the same profile within 10.6% in both cell lines and included genes with ≤2-fold expression changes throughout the time course (data not shown). Data were filtered further by eliminating those showing less than 2-fold expression changes at one or more points during the time course, resulting in a set of 1099 genes with a shared, significant profile. These represent 9% of the total number of genes on the microarray. The clustering of their expression data is common in both CCRF-CEM and HL-60 cells (Fig. 2a) and can be observed as a repeat pattern by comparing the seven columns on the left- and right-hand sides of the panel. The clustering algorithm also grouped activated and repressed genes separately. Since hyper-acetylation of histones facilitates de-repression of

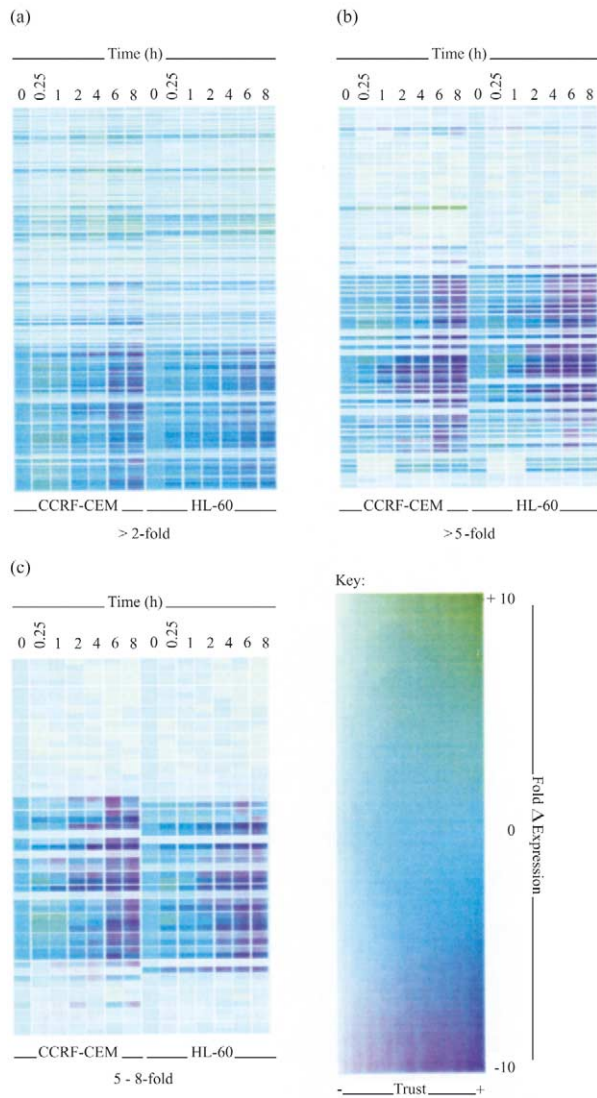


Fig. 2. Gene expression profiling of genes altered 2–8-fold in the temporal response of leukaemic cells to trichostatin A (TSA). (a) Cluster analysis of gene expression data from 1099 genes exhibiting changes in expression >2-fold over time. (b) Cluster analysis of gene expression data from 77 genes exhibiting changes in expression >5-fold over time. (c) Cluster analysis of gene expression data from 55 genes exhibiting changes in expression >5–8-fold over time. Hierarchical cluster analyses (\log_{10} of ratio, Pearson correlation) were performed on normalised, filtered gene data; all data were normalised to the corresponding data in the 0 h chip of the respective cell line, and only genes showing less than 10.6% variation in their expression profiles between cell lines during the time course, were included. A fold change expression level and data trust colour key is shown.

genes, we examined whether there were more genes upregulated than downregulated within the first 15 min. We found that the numbers were approximately equal; 28% upregulated and 25% downregulated (data not shown).

Of the 1099 genes displayed (Fig. 2a), 77 genes (representing 7% of those with a shared, significant profile, and 0.6% of the total genes represented on the GeneChip) were expressed >5-fold at one or more

points during the time course (Fig. 2b). Again, activated and repressed genes clustered separately and the patterns of gene expression on the two sides of the tree were repeated, indicating that these genes have a shared profile in the different cell lines. A subset of 55 genes, derived from the 77 gene set shown in Fig. 2b, exhibited 5- to 8-fold variation in expression and demonstrated the shared expression profiles of these genes between the two cell lines are demonstrated at a higher resolution (Fig. 2c).

3.4. The expression of a small number of trans-activating factors is highly sensitive to TSA

A limited number of genes (21) showed significant shared expression profiles with >8-fold changes in expression (Fig. 3). Over 50% of genes expressed >8-fold (12/21) were transcription factors or augmenters of transcription, and these made up an even higher proportion (67%; 8/12) of those altered in expression by over 10-fold. Ten of these transcription modulators are known to be involved in cancer, many are interlinked in their regulation and two pairs of genes which have the same chromosomal locus were found to be reciprocally regulated on histone hyper-acetylation.

The proto-oncogene *MYC* has been shown to be highly downregulated in response to TSA [18]. *MYC* is known to be overexpressed in many cancers [20], and is amplified in HL-60 cells [21]. Predictably, therefore, *MYC* was among the 21 genes with the most altered expression profiles (Figs. 3b and 4a). Interestingly, two genes which regulate the expression of *MYC* were also repressed. *ZNF278*, a hook zinc finger protein that is a transcriptional activator of *MYC* [22], and *NMI* which augments the transcriptional activation of *MYC* and is overexpressed in myeloid leukaemias [23], were both downregulated to low expression levels in response to TSA (Fig. 3a). Other downregulated proto-oncogenes included *MYB* (Fig. 3a) and *FLII*. The latter showed an initial repression followed by induction, before being rapidly downregulated between 6 and 8 h following treatment (Figs. 3b and 4a).

Two pairs of genes that occupy the same chromosomal region, were found to be reciprocally altered in their expression in response to TSA (Figs. 3b and 5b). The *HOXB6* gene, which was activated over 10-fold, maps to 17q21 as does *UBTF*, a gene that was repressed over 10-fold. In addition, *CDK10* and *CBFA2T3* which map very close to each other at 16q24 were highly activated and repressed, respectively (Figs. 3b and 5b).

3.5. Expression from an imprinted gene, *MKRN3* (*ZNF127*), is markedly inhibited in response to TSA

The most rapidly downregulated gene in this study was the paternally expressed imprinted gene *MKRN3*

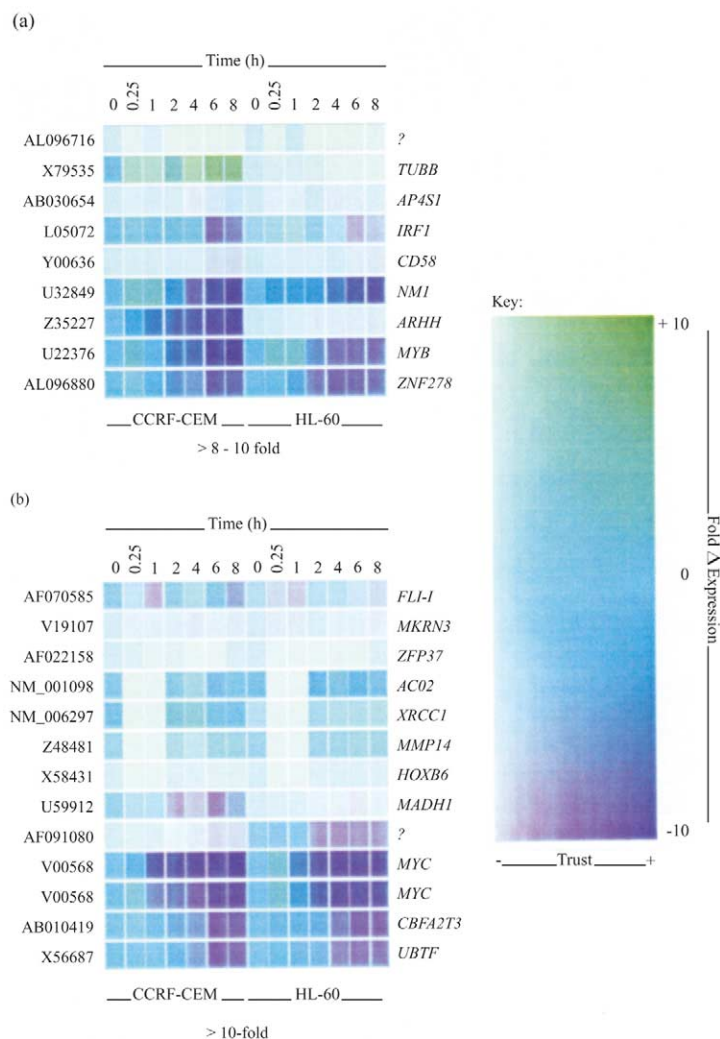


Fig. 3. Gene expression profiling of genes altered more than 8-fold in the temporal response of leukaemic cells to trichostatin A (TSA). (a) Cluster analysis of gene expression data from 9 genes exhibiting changes in expression >8–10-fold over time. (b) Cluster analysis of gene expression data from 12 genes exhibiting changes in expression >10-fold over time. Hierarchical cluster analyses (\log_{10} of ratio, Pearson correlation) were performed on normalised, filtered gene data; all data were normalised to the corresponding data in the 0 h chip of the respective cell line, and only genes showing less than 10.6% variation in their expression profiles between cell lines during the time course, were included. *MYC* is represented by two different probe sets corresponding to different regions of the same gene on the GeneChip microarray, the gene expression profiles of both are shown to illustrate reproducibility. Genes are labelled with HUGO approved gene names and GenBank accession numbers. Question marks indicate uncharacterised genes. A fold change expression level and data trust colour key is shown.

(*ZNF127*) involved in the Prader–Willi syndrome [24,25] which was repressed 7–10-fold within 15 min of TSA treatment (Fig. 3b). None of the other imprinted genes (*SNRPN*, *NDN*, *PAR-5* and *IPW*) clustered at this locus (15q11-13) had a significant or consistent response to histone hyper-acetylation (data not shown). Interestingly, a partially imprinted human gene, *IGRF2* [26], was also highly sensitive to histone hyper-acetylation and showed >10-fold activation in response to TSA (Fig. 5b).

3.6. TSA primary and secondary response genes can be distinguished by their expression profiles

Primary and secondary response genes were distinguished by their rates of change of expression. The

highest rate of change for primary activated genes occurred within the first fifteen minutes (Fig. 5), while transcripts corresponding to many secondary response genes continued to alter up to 8 h following treatment (Fig. 4).

Primary response genes were few in number, but showed very similar expression profiles (Fig. 5a). For analysis, data were restricted to genes with profiles that varied <10.6% between cell lines (see Section 2). Assuming that such stringent conditions might have eliminated important genes, the unrestricted data-set was re-examined and a further four genes with the same profile as those in the restricted data set were identified (Fig. 5b). All eight genes (Fig. 5) have disparate functions and chromosomal locations. Their rapid upregulation

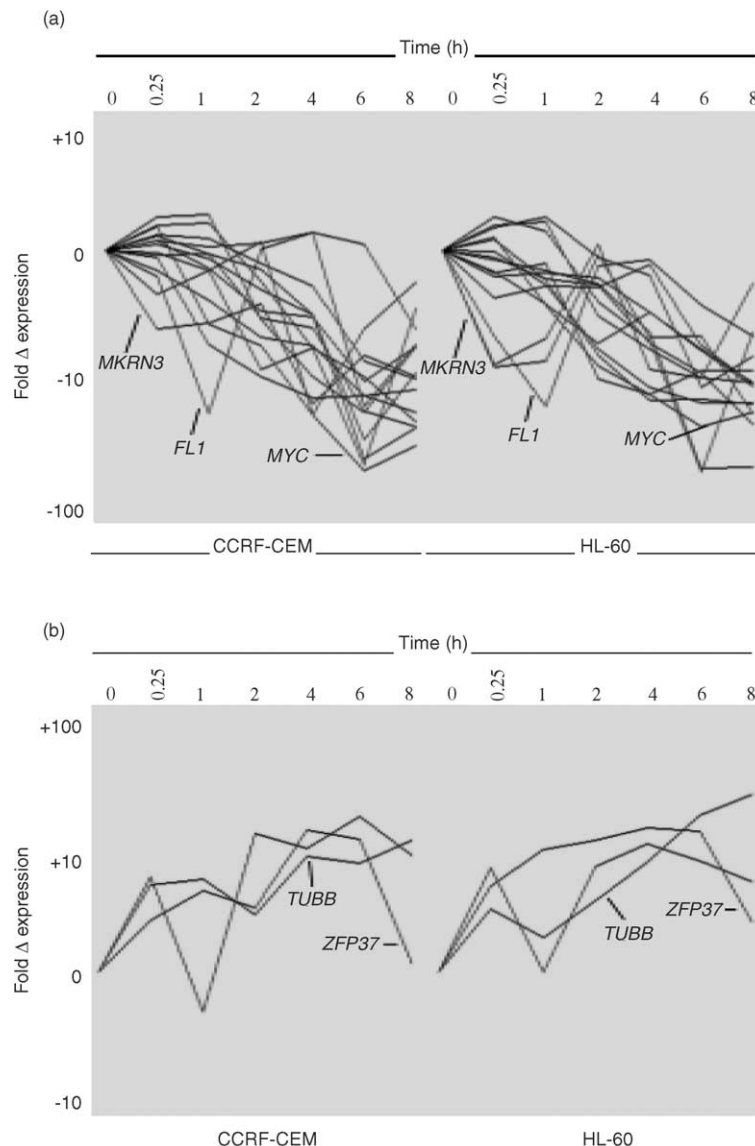


Fig. 4. Secondary response genes have distinctive expression profiles and a slower rate of change of expression. (a) Expression profiles of 14 downregulated genes (*MYC* is represented twice) derived from clusters (Fig. 3). (b) Expression profiles of 3 upregulated genes derived from clusters (Fig. 3). Log₁₀ of ratio data were plotted using GeneSpring 4.1. In response to TSA, the rate of change of expression of these genes was slower than that of primary response genes, although all had >8-fold expression changes. Over the 8 h period, more genes showed an overall pattern of down-regulation than upregulation. Individual genes are indicated by their HUGO approved gene names.

lation to high levels suggested that these are TSA primary response genes whose expression is altered as an immediate effect of histone hyper-acetylation. Contrary to these immediate early response genes, secondary response genes had a much slower rate of change of expression and repressed genes were often characterised by an initial lag phase (compare Figs. 4 and 5).

3.7. Verification of expression profiles of selected genes by real-time PCR

The responses of two genes to TSA were measured by quantitative PCR and in order to compare their profiles with similarly analysed microarray data. Fig. 6 shows

an analysis of triplicate data generated from individual PCR experiments compared with corresponding identically analysed microarray data (see Section 2). This comparison was intended to be qualitative rather than quantitative, since a correct quantitative fold-change comparison of PCR data and GeneSpring-analysed data would have required the PCR-generated data for each gene to be normalised to a panel of several invariant (TSA-insensitive) genes. The two genes chosen were *HOXB6* since it showed >10-fold activation, was a primary response, highly upregulated gene and was 'low trust' microarray data (Fig. 6a), and *NMI* since it was inactivated by >8-fold, was a secondary response gene, and was 'high trust' microarray data (Fig. 6b). At 0 h in

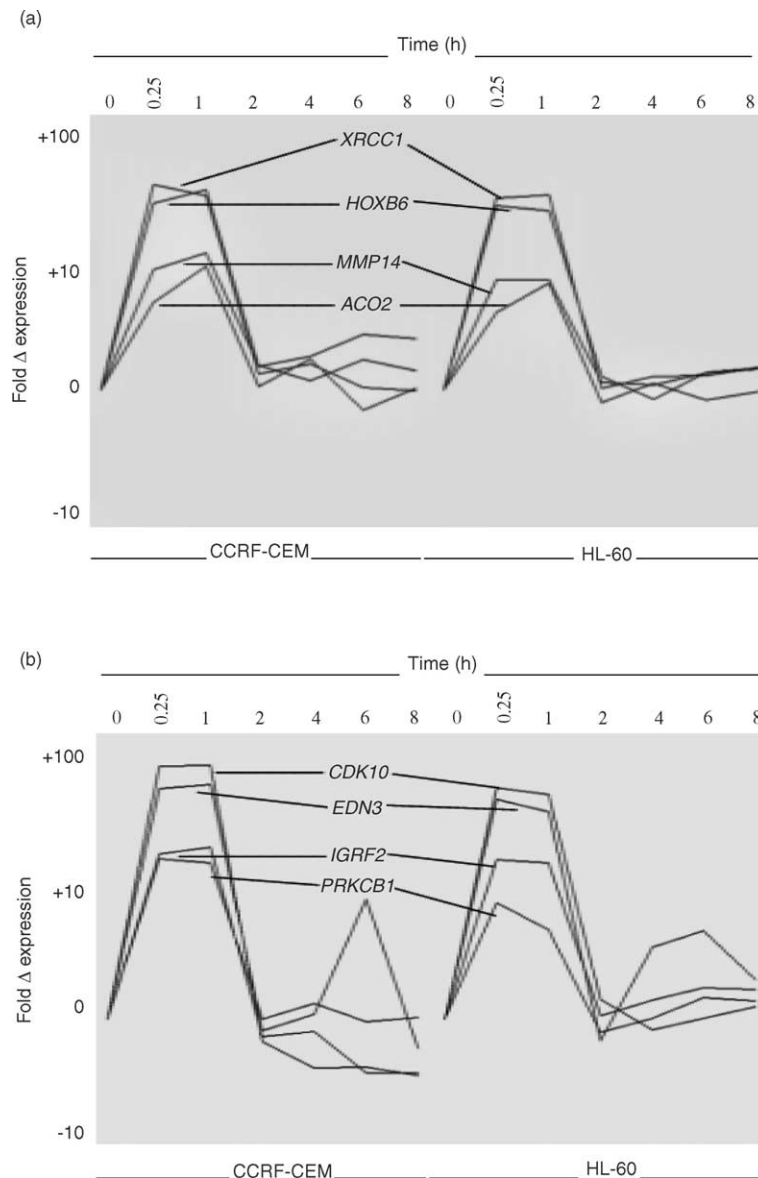


Fig. 5. Primary response genes have distinctive, shared expression profiles. (a) Expression profiles of four genes derived from the gene set shown in Fig. 3b. (b) Expression profiles of four genes derived from an unrestricted data-set. Eight genes showed a primary response to TSA and exhibited rapid upregulation to high levels of expression that were reduced to pretreatment levels within 2 h. Log₁₀ of ratio data were plotted using GeneSpring 4.1. Individual genes are indicated by HUGO approved gene names.

CCRF-CEM cells, *HOXB6* was undetectable, therefore both PCR and microarray data for *HOXB6* and *ACTB* were normalised to the lowest time point in the series (4 h) for comparison (upper panel, Fig. 6a). In HL-60 cells, microarray and PCR data for *HOXB6* and *ACTB* were normalised to the 0 h time point. For *NMI* comparison in HL-60 cells, microarray and PCR data were normalised to the 0.25 h time point (lower panel, Fig. 6b), and normalised to the 0 h time point in CCRF-CEM cells. Data were expressed as the ratio of the variant, TSA-sensitive gene (*HOXB6* or *NMI*) over the relatively non-variant gene (*ACTB*) to represent fold change of the variant gene relative to *ACTB*. Since the data in Fig. 6 are not expressed logarithmically, fluctuations

in expression corresponding to repression of the variant gene relative to *ACTB* are represented by values from 0 to 1 on the Y-axis, while values >1 represent induction. Repression is therefore compacted in Fig. 6. The profiles of microarray and PCR-generated data are similar in Fig. 6 suggesting that the data generated by GeneSpring microarray analysis for these two genes were a reliable reflection of gene activity. However, the fold induction or repression of the two genes in response to TSA did not directly relate to the corresponding fold change in Figs. 4 and 5. We believe that this is due in part to the fact that the *ACTB* gene varies in expression in response to TSA, thereby affecting the profile of any gene measured

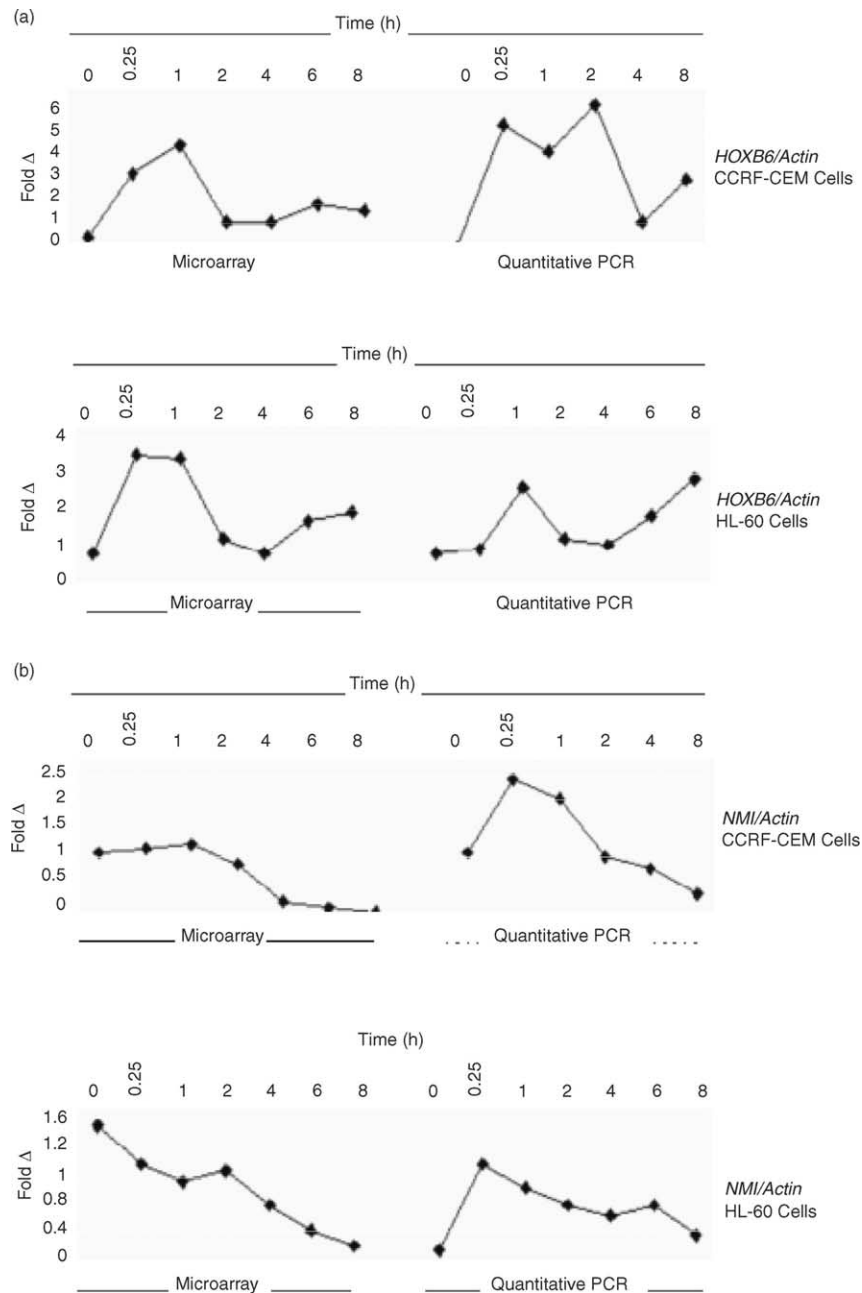


Fig. 6. Comparison of polymerase chain reaction (PCR) and microarray generated expression profiles for *HOXB6* and *NMI* genes. (a) Comparison of microarray expression profile for *HOXB6* with the corresponding PCR profile in CCRF-CEM and HL-60 cells. (b) Comparison of microarray expression profile for *NMI* with the corresponding quantitative PCR profile in CCRF-CEM and HL-60 cells. Identical aliquots of RNA from TSA-treated cells were used to generate the microarray and PCR data. Both sets of data were analysed identically and expressed as a ratio to *ACTB*. In the CCRF-CEM TSA time series, the 6 h time point was not represented in the PCR data, due to insufficient RNA. Triplicate (*HOXB6* or *NMI*) or duplicate (*ACTB*) data from real time PCR reactions were then averaged and normalised to one point in the time series of the respective cell line. Averaged, normalised *HOXB6* or *NMI* data were then normalised to similarly pre-normalised *ACTB* data (right-hand panels a and b). For accurate comparison, normalised *HOXB6* and *NMI* microarray data, were normalised to the corresponding *ACTB* microarray data (left-hand panels a and b). The profiles of microarray and PCR generated data were qualitatively similar.

against it in this type of PCR analysis. GeneSpring analysed microarray data were not subjected to this type of normalisation with the other genes. Indeed, differences in the fold change response of genes measured via microarray analysis and Real Time PCR have been noted by others [31].

4. Discussion

In this report, the functional link between histone acetylation and the expression profiles of approximately 12 000 genes was examined in two leukaemic cell lines using Affymetrix U95Av2 microarrays. The acetylation

induced by TSA observed in both cell types was similar to that shown in a previous report [18]. However, contrary to Van Lint and colleagues [18] who claimed that a small number of genes (2% of the genome) responded to TSA over an 8-h period, we found that the drug affected more genes (at least 9% of the genome; Fig. 2a). This is a conservative estimate since cell-type specific TSA gene responses have been excluded. The number of genes altered is not surprising given the pleiotropic effects of histone acetylation. The discrepancy (2% versus >9%) is likely to be due to the greater resolution of the microarray analysis compared with differential display PCR detection.

In addition to *MYC*, the gene response to TSA was consistent with the known effects of this anti-cancer drug to induce apoptosis and promote differentiation [27]. The activity of a number of interacting factors (*MYC*, *ZNF278*, *NMI*, *FLII*) was co-ordinately inhibited, as were genes involved in cell growth (*UBTF*, *MADH1*).

Histone hyper-acetylation inhibited transcription from the translocation breakpoint-associated gene *CBFA2T3* (*MTG16* or *MTGR2*) which encodes a zinc finger protein and is associated with a t(16;21) translocation that is a rare, but recurrent, chromosomal abnormality associated with therapy-related myeloid malignancies, involving fusion with the *RUNX1* gene. The *CBFA2T3* gene is related to *CBFA2T1* (*ETO*, *MTG8* or *AML1T1*), which also partners with *RUNX1* in the most common, t(8;21), acute myeloid leukaemia (AML) translocation, and to *CBFA2T2* (*MTGR1* or *EHT*) which contributes to the leukaemogenesis of t(8;21) AML by forming a complex with the RUNX1-CBFA2T1 fusion protein [28]. Notably, CBFA2T3 and related proteins (CBFA2T1 and CBFA2T2) are homologues of the *Drosophila* nervy protein [29] which is transcriptionally activated by the product of the homeotic gene *ultrabithorax* (*Ubx*). The human homologue of *Ubx* is *HOXB6*, one of the most highly and rapidly upregulated TSA-responsive genes (see Figs. 3b and 5a), raising the possibility that the inhibition of *CBFA2T3* could be linked to TSA-induced hyper-activation of *HOXB6*. *HOXB6* is not normally expressed in HL-60 cells and, unlike other *HOX* genes, is also not expressed during early haemopoiesis [30]. The hyper-acetylation response of *CBFA2T3* was not shared by the related genes *CBFA2T1* and *CBFA2T2* (data not shown).

A number of genes which were altered in expression by over 10-fold were in the same vicinity as those that had opposite regulatory profiles. At 17q21, the *UBTF* gene was inhibited while *HOXB6* was activated. A similar scenario was noted at 16q24 for *CBFA2T3* and *CDK10*, which were oppositely regulated in response to TSA. Other genes at 17q21 and at 16q24 were relatively insensitive to TSA indicating that the juxtaposition of

genes is not a reflection of their accessibility to changes in chromatin acetylation.

MKRN3 and *IGFR2* which are paternally and partially-maternally expressed imprinted genes, respectively [24,26], were oppositely regulated, but highly sensitive to histone hyper-acetylation. Once again, the lack of sensitivity of other genes in the same locality points towards a complex regulation of clustered genes. Indeed, the inhibition of *MKRN3* by TSA may be due to the activation of its anti-sense controlling transcript (*ZNF127AS*) via acetylation [24]. The repression of *MKRN3* in TSA-treated leukaemic cells may indicate inhibition of an aberrantly-activated developmental programme.

This study is limited by the number of genes represented on the microarray (12 000) and by the exclusion of cell type-specific data. Therefore, certain gene responses to TSA may remain undetected. Nevertheless, a group of genes have been identified that are highly sensitive to histone acetylation and have particular relevance to cancer and leukaemia. These can be grouped into those showing primary and secondary responses to TSA and many show a high potential for interlinked regulation. The identification of genes that are consistently TSA-sensitive in aetiologically disparate leukaemias may provide key targets for future therapeutic intervention.

Acknowledgements

The Joint Research Board of St Bartholomew's Hospital and The St Bartholomew's and Royal London Charitable Foundation are gratefully acknowledged for financial support.

References

1. Kuo M-H, Allis CD. Roles of histone acetyltransferases and deacetylases in gene regulation. *BioEssays* 1998, **20**, 615–626.
2. Gray SG, Ekstrom TJ. The human histone deacetylase family. *Exp Cell Res* 2001, **262**, 75–83.
3. Pandolfi PP. Transcription therapy for cancer. *Oncogene* 2001, **20**, 3116–3127.
4. Minucci S, Nervi C, Lo Coco F, Pelicci PG. Histone deacetylases: a common molecular target for differentiation treatment of acute myeloid leukemias? *Oncogene* 2001, **20**, 3110–3115.
5. Lin RJ, Nagy L, Inoue S, Shao W, Miller Jr WH, Evans RM. Role of the histone deacetylase complex in acute promyelocytic leukaemia. *Nature* 1998, **391**, 811–814.
6. Saunders N, Dicker A, Popa C, Jones S, Dahler A. Histone deacetylase inhibitors as potential anti-skin cancer agents. *Cancer Res* 1999, **59**, 399–404.
7. Glick RD, Swendeman SL, Coffey DC, et al. Hybrid polar histone deacetylase inhibitor induces apoptosis and CD95/CD95 ligand expression in human neuroblastoma. *Cancer Res* 1999, **59**, 4392–4399.
8. Vigushin DM, Ali S, Pace PE, et al. Trichostatin A is a histone deacetylase inhibitor with potent antitumor activity against breast cancer in vivo. *Clin Cancer Res* 2001, **7**, 971–976.

9. Magnaghi-Jaulin L, Groisman R, Naguibneva I, et al. Retinoblastoma protein represses transcription by recruiting a histone deacetylase. *Nature* 1998, **391**, 601–605.
10. Zhang Y, Ng HH, Erdjument-Bromage H, Tempst P, Bird A, Reinberg D. Analysis of the NuRD subunits reveals a histone deacetylase core complex and a connection with DNA methylation. *Genes Dev* 1999, **13**, 1924–1935.
11. Wang J-H, Hoshino T, Redner RL, Kajigaya S, Liu JM. ETO, fusion partner in t(8:21) acute myeloid leukaemia, represses transcription by interaction with the human N-coR/mSin3/HDAC1 complex. *Proc Natl Acad Sci USA* 1998, **95**, 10860–10865.
12. Wang J-H, Avitahl N, Cariappa A, et al. Aiolos regulates B cell activation and maturation to effector state. *Immunity* 1998, **9**, 543–553.
13. Sun L, Heerema N, Crotty L, et al. Expression of dominant-negative and mutant isoforms of the antileukemic transcription factor Ikaros in infant acute lymphoblastic leukemia. *Proc Natl Acad Sci USA* 1999, **96**, 680–685.
14. Sun L, Crotty ML, Sensel M, et al. Expression of dominant-negative Ikaros isoforms in T-cell acute lymphoblastic leukemia. *Clin Cancer Res* 1999, **5**, 2112–2120.
15. Winandy S, Wu P, Georgopoulos K. A dominant mutation in the Ikaros gene leads to rapid development of leukaemia and lymphoma. *Cell* 1995, **83**, 289–299.
16. Banerjee S, Bennion GR, Goldberg MW, Allen TD. ATP dependent histone phosphorylation and nucleosome assembly in a human cell-free extract. *Nucl Acids Res* 1991, **19**, 5999–6006.
17. Bonner WM, West MHP, Stedman JD. Two-dimensional gel analysis of histones in acid extracts of nuclei, cells, and tissues. *Eur J Biochem* 1980, **109**, 19–23.
18. Van Lint C, Emiliani S, Verdin E. The expression of a small fraction of cellular genes is changed in response to histone hyperacetylation. *Gene Exp* 1996, **5**, 245–253.
19. Yoshida M, Kijima M, Akita M, Beppu T. Potent and specific inhibition of mammalian histone deacetylase both in vivo and in vitro by Trichostatin A. *J Biol Chem* 1990, **265**, 17174–17179.
20. He TC, Sparks AB, Rago C, et al. Identification of c-MYC as a target of the APC pathway. *Science* 1998, **281**, 1438–1441.
21. Collins S, Groudine M. Amplification of endogenous myc-related DNA sequences in a human myeloid leukaemia cell line. *Nature* 1982, **298**, 679–681.
22. Kobayashi A, Yamagiwa H, Hoshino H, et al. A combinatorial code for gene expression generated by transcription factor Bach2 and MAZR (MAZ-related factor) through the BTB/POZ domain. *Mol Cell Biol* 2000, **20**, 1733–1746.
23. Bao J, Zervos AS. Isolation and characterization of Nmi, a novel partner of Myc proteins. *Oncogene* 1996, **12**, 2171–2176.
24. Jong MT, Gray TA, Ji Y, et al. A novel imprinted gene, encoding a RING zinc-finger protein, and overlapping antisense transcript in the Prader–Willi syndrome critical region. *Hum Mol Genet* 1999, **8**, 783–793.
25. Nicholls RD, Saitoh S, Horsthemke B. Imprinting in Prader–Willi and Angelman syndromes. *Trends Genet* 1998, **14**, 194–200.
26. Wutz A, Smrzka OW, Schweifer N, Schellander K, Wagner EF, Barlow DP. Imprinted expression of the Igf2r gene depends on an intronic CpG island. *Nature* 1997, **389**, 745–749.
27. Marks PA, Richon VM, Breslow R, Rifkind RA. Histone deacetylase inhibitors as new cancer drugs. *Curr Opin Oncol* 2001, **13**, 477–483.
28. Kitabayashi I, Ida K, Morohoshi F, et al. The AML1-MTG8 leukemic fusion protein forms a complex with a novel member of the MTG8(ETO/CDR) family, MTGR1. *Mol Cell Biol* 1998, **18**, 846–858.
29. Calabi F, Cilli V. CBFA2T1, a gene rearranged in human leukaemia, is a member of a multigene family. *Genomics* 1998, **52**, 332–341.
30. Sauvageau G, Lansdorp PM, Eaves CJ, et al. Differential expression of homeobox genes in functionally distinct CD34+ subpopulations of human bone marrow cells. *Proc Natl Acad Sci USA* 1994, **91**, 12223–12227.
31. Rajeevan MS, Ranamukhaarachchi DG, Vernon SD, Unger ER. Use of real-time quantitative PCR to validate the results of cDNA array and differential display PCR technologies. *Methods* 2001, **25**, 443–451.